

Niobium- and titanium-based coating for the protection of carbon steel SAE 1020 against corrosion

Rodrigo Helleis, Guilherme Arielo Rodrigues Maia and Eryza Guimarães de Castro

Department of Chemistry, Midwest State University (UNICENTRO), Guarapuava, Brazil

Larissa Oliveira Berbel and Isolda Costa

Materials Science and Technology Center, Nuclear and Energy Research Institute (IPEN), São Paulo, Brazil, and

Everson do Prado Banczek

Department of Chemistry, Midwest State University (UNICENTRO), Guarapuava, Brazil

Abstract

Purpose – The purpose of this paper is to evaluate the protection against corrosion of carbon steel SAE 1020 promoted by a niobium- and titanium-based coating produced from a resin obtained by the Pechini method.

Design/methodology/approach – A resin was prepared with ammonium niobium oxalate as niobium precursor and K_2TiF_6 as titanium precursor. Carbon Steel SAE 1020 plates were dip coated in the resin and calcinated for 1 h at 600 °C. Scanning electron microscopy, energy dispersive spectroscopy and X-ray diffraction were used to characterize the coating morphologically and structurally. Open circuit potential, electrochemical impedance spectroscopy, anodic potentiodynamic polarization and scanning vibrating electrode technique were used to evaluate the corrosion protection of the coating.

Findings – The electrochemical analyses evidence slight protection against corrosion of the coating by itself; however, the needle-like crystal structure obtained may potentially provide a good anchorage site, suggesting the coating could be used as a pretreatment that may present similar application to phosphating processes, generating lower environmental impacts.

Originality/value – Due to increasingly restrictive environmental laws, new environmentally friendlier surface treatments must be researched. This paper approaches this matter using a combination of niobium- and titanium-based coating, produced by a cleaner process, the Pechini method.

Keywords Electrochemistry, Pechini method, Pretreatment

Paper type Research paper

1. Introduction

Carbon steel is widely used in the industry due to its excellent mechanical properties and low cost. In contrast, it resists poorly to corrosion, which results in the necessity of surface treatment even in mildly corrosive environments (Kim *et al.*, 2017). Every year, corrosion in pipelines and equipment account for economic losses in the order of hundreds of billions of dollars and even human casualties in production plants; this combined with the increasing awareness for environmental issues rises the importance of the study in new, cleaner and effective ways of protection against corrosion (Hou *et al.*, 2016; Matos *et al.*, 2018). Phosphating is one of the surface treatments most commonly used by the industry to protect metallic materials against corrosion, but the process generates toxic waste that is difficult to treat. The toxicity is related to the addition of nickel in the phosphating bath and the use of hexavalent chromium as sealer (Banczek *et al.*, 2010).

Metals such as niobium and titanium are naturally resistant to corrosion, as they form a dense layer of oxides on the surface that serves as a barrier. This, allied to their mechanical properties, makes these metals, materials of interest in the biomedical area for implants. This is due to their great biocompatibility and the hindering of the attack from corrosive body fluids, arising as a potential less toxic alternative to traditional surface treatments (McMahon *et al.*, 2012; Pradhan *et al.*, 2016; Detlinger *et al.*, 2019). Taking that into consideration and knowing that surface coatings are used to improve corrosion resistance. Being able to artificially deposit niobium and titanium oxides on the surface of carbon steel may potentially protect it against corrosion (Nazeer and Madkour, 2018).

The oxides can be deposited on the surface of metallic material by different techniques such as chemical vapor deposition, physical vapor deposition and the sol-gel method

The current issue and full text archive of this journal is available on Emerald Insight at: <https://www.emerald.com/insight/0003-5599.htm>



Anti-Corrosion Methods and Materials
© Emerald Publishing Limited [ISSN 0003-5599]
[DOI 10.1108/ACMM-10-2021-2561]

This study was financed in part by the Coordenação de Aperfeiçoamento de Pessoal de Nível Superior – Brasil (CAPES) – Finance Code 001. The authors are also grateful to CNPq and Fundação Araucária for the financial support and Companhia Brasileira de Metalurgia e Mineração (CBMM) for providing the ammonium niobium oxalate used as precursor.

Received 27 October 2021

Revised 22 April 2022

Accepted 27 April 2022

(Pan *et al.*, 2016). The Pechini method, or polymeric precursor method, derives from the sol-gel method and consists in the preparation of a resin by reacting a chelating agent and the metallic precursor. A polyalcohol is added to the metallic chelate, causing a polyesterification reaction, immobilizing the metallic cation in the structure. The resin is then calcinated to remove the organic matter and form the desired oxide. This method presents the advantages of using relatively low temperature, the possibility of large-scale production, low toxicity and relatively low costs (Dias *et al.*, 2018; Trino *et al.*, 2018; Detlinger *et al.*, 2019; Tractz *et al.*, 2021).

Niobium oxide and titanium oxide were studied separately in the literature. A niobium oxide coating produced by the Pechini method for the protection of carbon steel against corrosion was studied by Detlinger *et al.* (2020). The results showed higher corrosion resistance of the coated plates when comparing to the bare substrate, obtaining better results with lower ethylene glycol (EG)/citric acid ratio, as the amount of niobium on the surface decreases with the increase of the ratio. The use of titanium dioxide thin films deposited by sputtering for the protection against corrosion of stainless steel was evaluated by Hartwig *et al.* (2017). The coatings obtained exhibit great corrosion protection and the increase of the coating thickness decrease its protection. This is due to the increase on the roughness and donor density of the coating that affects the electrochemical behavior of the coated substrate.

Considering the above-mentioned, the aim of the study is to produce and characterize, morphologically, structurally and electrochemically, a niobium and titanium coating for protection of carbon steel (SAE 1020) against corrosion.

2. Materials and methods

2.1 Resin preparation

The resin was prepared by the methodology described by Detlinger and co-workers (Detlinger *et al.*, 2019), using citric acid (CA, 99.89%, Neon) as chelating agent, EG (99.95%, PanReac AppliChem) as polyalcohol, ammonium niobium oxalate ($\text{NH}_4[\text{Nb}(\text{C}_2\text{O}_4)_2(\text{H}_2\text{O})]\cdot\text{H}_2\text{O}$, CBMM) as niobium precursor and potassium hexafluorotitanate (K_2TiF_6 , Sigma-Aldrich) as titanium precursor. The used molar ratios were EG/AC/Nb/Ti: 8/1/0.1/0.06. Citric acid was added to EG at 60°C under constant agitation until complete dissolution followed by the addition of the metal precursor until complete dissolution at 60°C, then the reaction was carried for 1 h under constant agitation at 60°C.

2.2 Coating preparation

Carbon steel (SAE, 1020) plates with the size of 2×2 cm were sanded with silicon carbide sand paper with progressive grades of #200, #320, #400, #600 and #1200 to remove all impurities from the surface of the material. The sanded plate was immersed in the resin for 15 min, then hanged to drain the excess of resin for 5 min followed by the calcination of the plates at 600°C for 1 h in a preheated muffle furnace. After calcination, the plates were cleaned with a soft bristle paint-brush, rinsed with deionized water and dried to remove the organic material left.

2.3 Morphologic and structural characterization

Scanning electron microscopy (SEM) images were obtained using a Tescan® Vega3 equipment to visualize the morphology of the metallic surface as well as the coatings; the equipment was coupled with an energy dispersive spectroscopy (EDS) that was used to determine the elemental composition of the coating.

X-ray diffraction (XRD) was used to identify the crystallinity of the coating, as well as the phases formed after the calcination process. The equipment used was a Rigaku Multiflex diffractometer using a $\text{CuK}\alpha$ ($\lambda = 1.5418 \text{ \AA}$) radiation, power of 40 mV and current of 20 mA, scanning in the range of 10° – 80° with a step of 0.06° and a speed of 1° min^{-1} .

2.4 Electrochemical analyses

For the electrochemical characterization, a three-electrode electrochemical cell was used, where the working electrode was the coated or uncoated plate of carbon steel (contact area of 0.78 cm^2), the counter electrode was a helical wire of metallic platinum, the reference was an Ag/AgCl electrode and the electrolyte solution used was $\text{NaCl } 0.5 \text{ mol L}^{-1}$.

A Gamry PC4-300/EIS300 potentiostat was used for the electrochemical analysis at the temperature of $20 \pm 2^\circ\text{C}$. Electrochemical impedance spectroscopy (EIS) measurements were performed potentiostatically at open circuit potential (OCP) with perturbation amplitude of $\pm 10 \text{ mV}$, the frequency range of 10 kHz to 10 mHz and the acquisition of 10 points per decade. The EIS equivalent circuit fittings were obtained using the Gamry Instruments EchemAnalyst™ software. Anodic potentiodynamic polarization measures were carried from the OCP, with a stabilization time of 8,000 s, to an overvoltage of +500 mV using a scanning rate of $+10 \text{ mV s}^{-1}$.

The scanning vibrating electrode technique (SVET) analysis was performed in an Applicable Electronics™ equipment controlled by an ASET 4.0 software, using an insulated Pt-Ir probe with platinum black deposited on the tip as a vibrating electrode. The vibrating electrode was placed $100 \mu\text{m}$ above the surface and the amplitude of vibration was $19 \mu\text{m}$, vibration frequencies of the probe were 174 Hz (X) and 73 Hz (Z). All experiments were performed in a Faraday cage at $20 \pm 2^\circ\text{C}$. Scanning was carried out over the exposed area (0.25 cm^2). Experiments were performed using 5 mmol L^{-1} NaCl solution for a period of 24 h and the maps were obtained every 2 h. During the interval between the SVET measurements, optical microscope images were obtained *in situ* on the surface of the coated material.

3. Results and discussion

3.1 Morphologic and structural characterization

SEM micrographs for the bare substrate and the coated material were obtained to observe the surface of the samples. The images are depicted in Figures 1 and 2, respectively. The bare material was smooth with little defects, probably due to the sanding process. Conversely, the coating that was deposited on the surface of the metallic material using the Pechini method was rough and non-homogenous. Under higher magnification, a needle-like crystal structure was identified, as shown in Figure 3. Similar crystals were observed in the literature for a Nb_2O_5 coating in carbon steel prepared by the Pechini method (Rodrigues *et al.*, 2014) and for niobium oxide deposits

Figure 1 Scanning electron micrograph for the uncoated steel under 1,000 times magnification

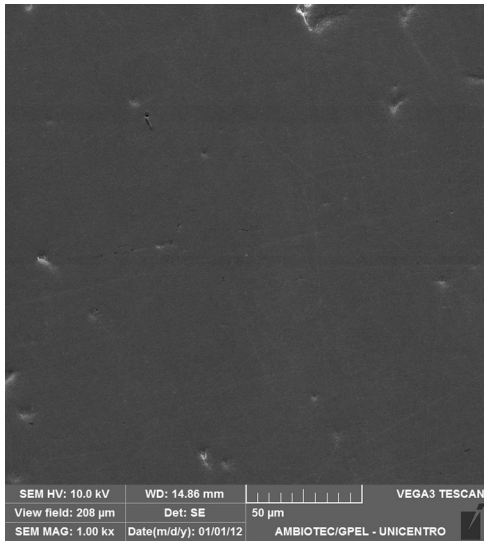
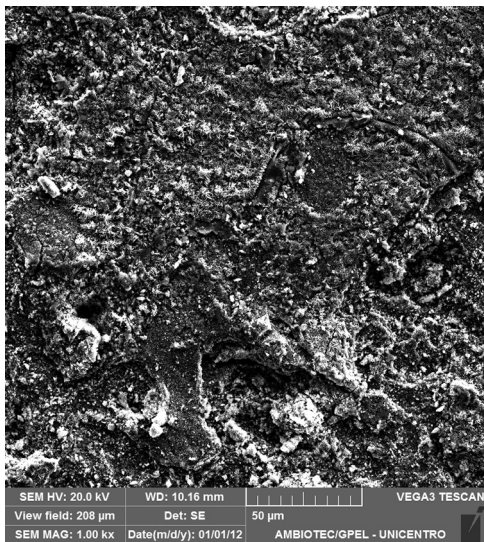


Figure 2 Scanning electron micrograph for the coated steel under 1,000 times magnification



generated after immersion in NaOH and H₂SO₄ solutions (Chukwuike *et al.*, 2021). The presence of the crystals on the material surface broadens the potential applications of the coating. Phosphating baths form crystals on the surface, with different morphologies depending on the formed phosphate, which serve as an anchorage site for further treatments (Banczek *et al.*, 2010). Banczek *et al.* (2009) found needle-like structures when studying phosphating baths with zinc. Therefore, a similar application, as pretreatment, is possible for the obtained coating.

The weight percentage of the elements on the surface, obtained by EDS, is presented in Table 1. Fe, O, Nb, Ti and K were found on the surface, the presence of K could indicate residual elements of the titanium precursor (K₂TiF₆) or the

Figure 3 Scanning electron micrograph showing the needle structure on the coated steel under 10,000 times magnification

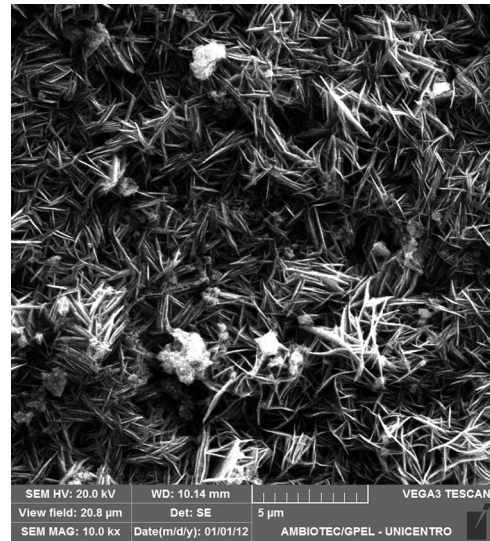


Table 1 Semi-quantitative EDS elemental analysis of coated steel

Element	Fe	O	Nb	Ti	K
Weight %	65.47	30.95	1.18	0.45	1.96

formation of phases other than niobium and titanium oxides, as its concentration was higher in comparison to Nb and Ti. Although, due to the semi-quantitative nature of the EDS elemental analyses there may be a variation of the percentages. The EDS maps are shown in Figure 4, a homogenous distribution of the elements was observed, making it difficult for galvanic corrosion caused by a difference in the elements concentrations to happen.

XRD was used to identify the phases of the resin calcinated powder, as shown in Figure 5. As can be seen in this Figure, the diffractogram presents characteristics of low crystallinity materials, with low intensity peaks. Furthermore, the large

Figure 4 EDS element distribution maps for the coated steel

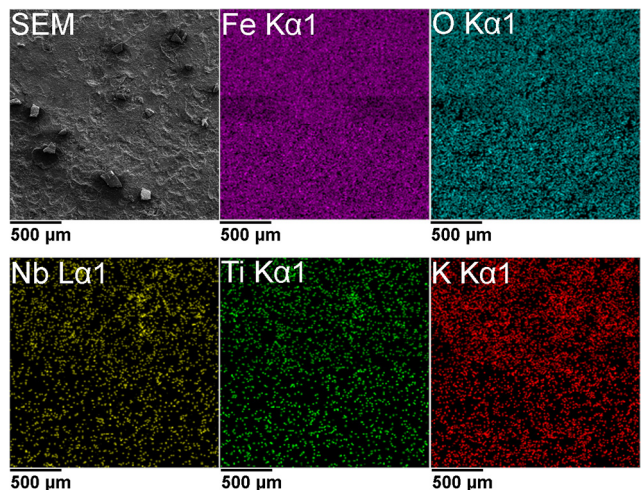
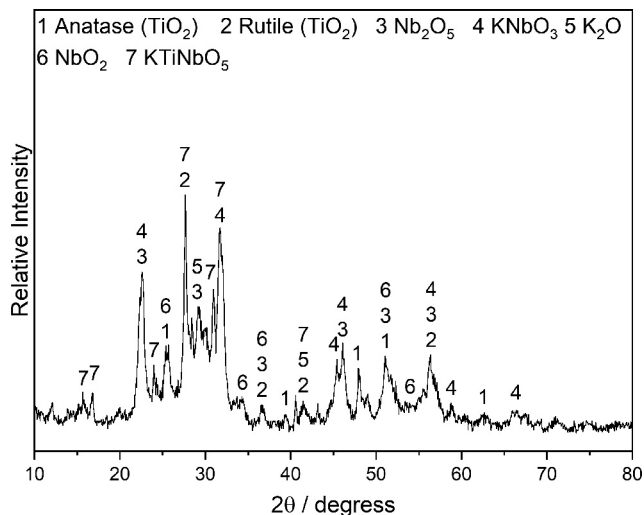
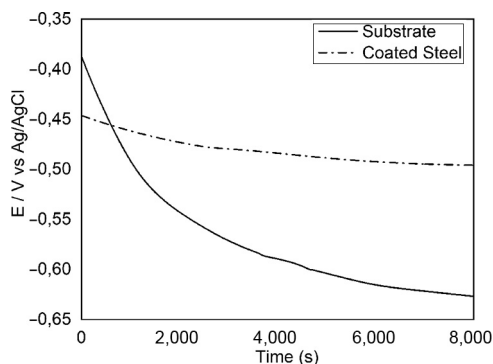


Figure 5 X-ray diffractogram for the resin powder

number of diffraction peaks suggests the formation of a mixture of phases among which TiO_2 (anatase and rutile), Nb_2O_5 , KNbO_3 , K_2O , NbO_2 and KTiNbO_5 stand out. These phases often present peaks at the same position in the diffractogram, as indicated in [Figure 5](#). For this reason, the exact identification of the phases present in the material is difficult. The possible presence of TiO_2 , NbO_2 , Nb_2O_5 and insoluble salts such as KNbO_3 could indicate a coating with good corrosion protection properties, as they are corrosion resistant agents ([Tao et al., 2014](#); [Tegner et al., 2015](#); [Detlinger et al., 2019](#); [Detlinger et al., 2020](#); [Santos Júnior et al., 2022](#)).

3.2 Electrochemical characterization

Open circuit potential curves for the substrate and the coated steel were obtained to evaluate their respective electrochemical behavior, as can be seen in [Figure 6](#). The values of potential decreased with time, suggesting the dissolution of the oxide layer formed, followed by the activation of the surface which stabilized the system ([Robin, 2004](#); [Sowa et al., 2016](#)). The coated steel stabilized at a higher potential than the substrate, indicating a higher nobility of the coated surface, suggesting a corrosion protection on the coated material ([Pillís et al., 2016](#); [Li et al., 2017](#); [Helleis et al., 2021](#)). A lower variation in the coated carbon steel potential was observed, suggesting a higher

Figure 6 OCP curves for the substrate and coated steel

stability of the formed oxides, indicating a higher resistance to corrosion for the material. This behavior was verified by the potential stability from the first moments of immersion. [Santos Júnior et al. \(2022\)](#), related the potential stabilization promoted by niobates obtained in the surface of metallic niobium samples, evidencing the stability of the obtained coating.

The anodic polarization curves depicted in [Figure 7](#) supported the results of the OCP, as the coated steel curve was shifted to lower current densities and higher potential values, when compared to the substrate indicating the suppression of the anodic dissolution of carbon steel and suggesting that the coated steel was protected against corrosion near the corrosion potential ([Frag et al., 2015](#); [Cui et al., 2016](#); [Zhao et al., 2017](#); [Detlinger et al., 2019](#); [Zhang et al., 2019](#)). In the potential region in the studied electrolyte, a passive behavior was not observed for both the coated and uncoated samples. For the uncoated carbon steel, this behavior was related to the electrochemical activity promoted by the anodic polarization. This activity is characteristic of the substrate, presenting low corrosion resistance. For the coated samples, the active behavior can be explained by the ionic conduction capacity by the movement of interlayer cations of the oxide, as related in the literature ([Im et al., 2014](#)).

EIS measurements for the substrate and coated carbon steel were conducted to better understand the kinetics of the corrosive process in the system. The curves obtained are presented in [Figures 8, 9](#) and [10](#). The Nyquist plot, in [Figure 8](#), showed a complete capacitive arc for the substrate and an incomplete arc for the coated steel, similar to the capacitive arcs found in the literature for a niobium pentoxide coating obtained using magnetron sputtering on AISI 316 Stainless Steel ([Pillís et al., 2016](#)). The larger radius of the capacitive arc for the coated surface, when extrapolated to regions of lower frequencies, was associated to higher values of impedance, suggesting a delay in the charge transfer reactions and higher corrosion resistance ([Pillís et al., 2016](#); [Detlinger et al., 2019](#)). Bode phase angle plots, shown in [Figure 9](#), depicted one time constant for both the substrate and the coated carbon steel,

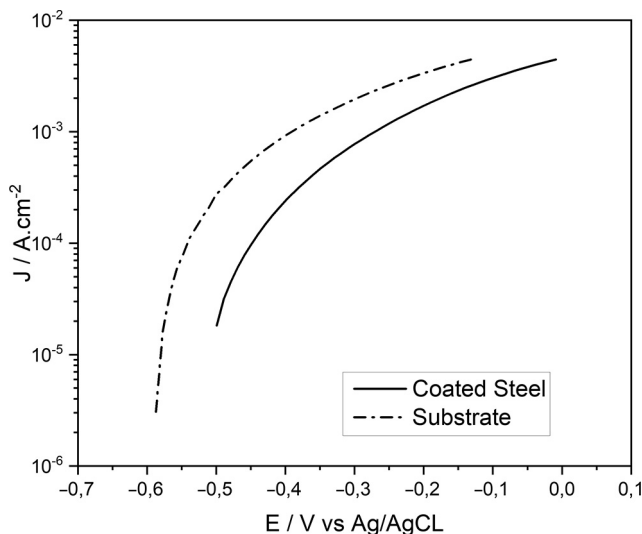
Figure 7 Potentiodynamic anodic polarization curves for the substrate and coated steel

Figure 8 EIS Nyquist plots for the substrate and coated steel

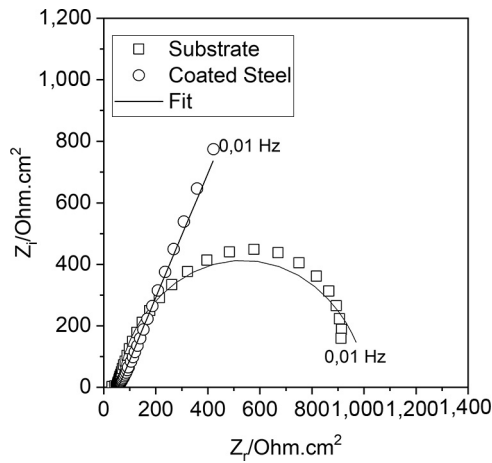


Figure 9 EIS phase angle Bode plots for the substrate and coated steel

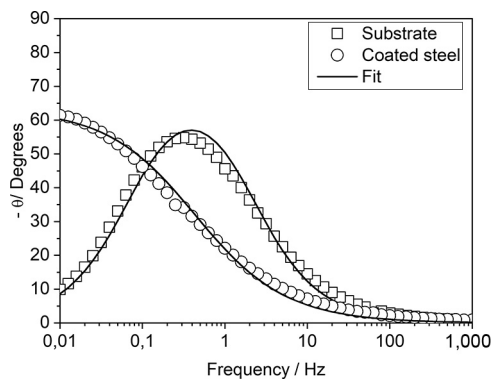
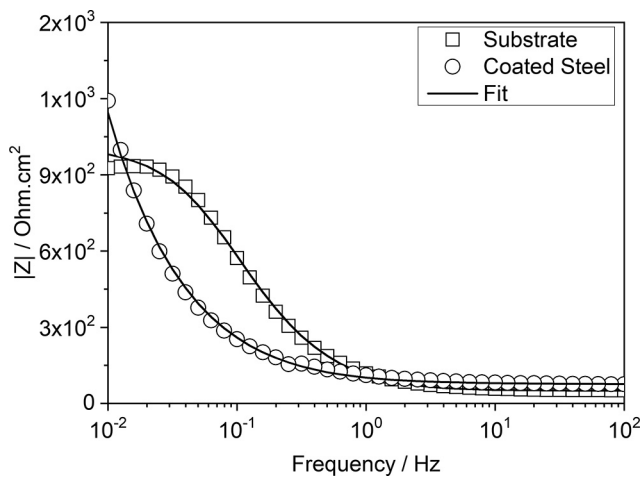


Figure 10 EIS impedance modulus Bode plots for the substrate and coated steel



contrarily to the expected two-time constants for the coated sample. Similar results in the literature were found for niobium carbide coatings on carbon steel SAE 1045 (Orjuela *et al.*, 2014) and for a niobium oxide coating on carbon steel SAE

1020 (Detlinger *et al.*, 2019). The single time constant of the coated steel sample in the Bode plot presented a higher phase angle and was shifted towards regions of lower frequencies, indicating an enhancement in the corrosion protection of the system (Orjuela *et al.*, 2014; Detlinger *et al.*, 2019). The Bode impedance modulus plots seen in Figure 10 showed that in regions of higher frequencies there was no impedance response, and a higher value of impedance modulus for the coated material in regions of lower frequencies, suggesting a surface that was resistant to the electrolyte solution attack and, consequently, a better corrosion resistance than the uncoated material (Detlinger *et al.*, 2019)

Dielectric behavior of the coating could be related to the EIS results, due to the presence of niobium in different oxidation states (Nb^{4+} and Nb^{5+}), as suggested by the peaks related to NbO_2 , Nb_2O_5 and $KNbO_3$ in Figure 5. In regions of higher frequencies, representing the interaction between electrolyte and coating, the capacitances behaved as a short circuit, permitting the passage of current to the substrate, there being no impedance response. In lower frequencies regions, representing the interaction between the surface of the coating (and its defects) and the electrolyte, the capacitances behaved as an open circuit. The defects resistance and the charge transfer resistance act on the system resulting in an impedance response (Orjuela *et al.*, 2014; Chukwuike *et al.*, 2021). The lack of impedance response in higher frequencies made the capacitive arc in the Nyquist plot incomplete, hid the higher frequency time constant expected on the Bode phase angle plots and also hid the increase of impedance modulus in higher frequencies on the Bode impedance modulus plot for the coated steel.

The EIS data was fitted using an equivalent circuit, depicted in Figure 11. With the fitted curves, values for the electrolyte resistance (R_{sol}), the charge transfer resistance (R_{ct}) and the constant phase element (CPE) were obtained. The results are shown in Table 2. A CPE was chosen for the equivalent circuit due to the nonideality the system, and a value for n was also obtained, referring to the ideality of the capacitor. The value for n varies between 0 and 1, when $n = 1$, it represents a pure capacitive behavior, while, when $n = 0$, it represents a pure resistive behavior (Cui *et al.*, 2017a; Liu *et al.*, 2021). The magnitude of the value of n for the coated sample is similar to a zinc phosphate conversion coating on carbon steel SAE 1020 studied by Huang *et al.* (2019) and to a europium oxide-based conversion coating studied by Mofidabadi *et al.* (2021). The reduction in the value of n for the coated sample suggests a coating with a rough, heterogenous surface, in contrast to the smoother, more homogenous surface of the bare material, evidenced by a higher value of n . These results can be verified

Figure 11 Equivalent circuit used for fitting the experimental EIS data

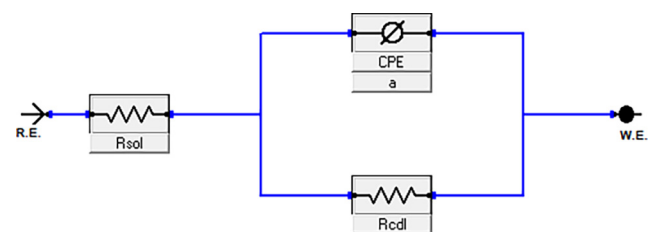


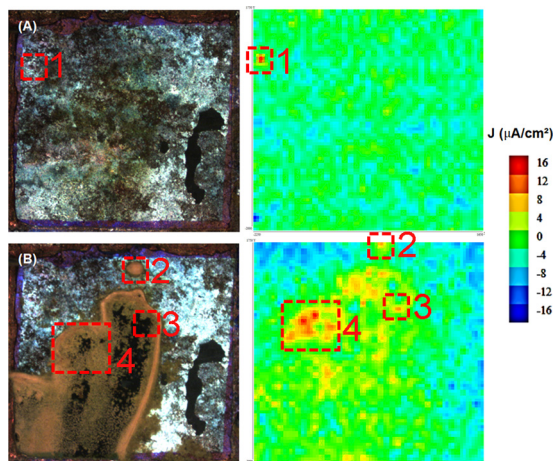
Table 2 EIS parameters for the bare substrate and coated steel

Sample	R_{sol} (Ω cm ²)	R_{ct} (Ω cm ²)	CPE (S s ⁿ cm ⁻²)	n
Substrate	50.26 ± 0.24	967.3 ± 9.84	2.07 E ⁻³ ± 1.75 E ⁻⁴	0.90
Coated steel	56.21 ± 0.25	1.86 E ⁵ ± 7.17 E ³	8.67 E ⁻³ ± 7.02 E ⁻⁵	0.71

by the micrographs seen in Figures 1 and 2 (Mofidabadi *et al.*, 2021). The values obtained for the R_{sol} were similar in magnitude for the coated and uncoated material, showing that the electrolytes used in both analyses did not vary significantly, presenting similar conductivity (Cui *et al.*, 2017b). R_{ct} results showed a great difference in value between the samples. The coated plate charge transfer resistance was significantly higher than the resistance for the substrate, indicating a higher corrosion resistance for the coated plate. These results confirmed the qualitative visual analysis of the Nyquist and Bode plots in Figures 8 to 10, and also corroborate to the results obtained by the OCP curves in Figure 6 and potentiodynamic polarization curves in Figure 7.

The local corrosion of the material was evaluated using SVET, as shown in Figure 12. The maps obtained presents anodic regions in red and cathodic regions in blue. After 2 h of immersion [Figure 12 (A)], an active region, was observed, indicating the formation of a pit before it was visible in the micrograph. This result could be related to a possible defect or crack on the coating, which could be a problem when using the material as a surface treatment by itself. After 24 h of immersion [Figure 12 (B)] it was possible to visualize the deposition of corrosion products on the surface of the material. An overall increase in the current density was observed, indicating a coating that was not passive. The highlighted areas showed the formation of pits on the surface, suggesting a non-homogenous coating with defects, as some regions were attacked and others remained protected. This result suggested that the coating might not be best used as a surface treatment by itself, but due to its morphology, as seen in Figures 2 and 3, it could be used in conjunction with other surface treatments (Ferreira *et al.*, 2022).

Figure 12 SVET maps and optical micrographs of the coated carbon steel: (A) after 2 hours of immersion; (B) after 24 hours of immersion



4. Conclusion

The deposition of a niobium- and titanium-based coating on carbon steel SAE 1020 provided slight protection against corrosion for the material. OCP, anodic polarization and EIS analyses indicated higher corrosion protection for the coated carbon steel than the bare substrate, whereas SVET showed a non-homogenous coating with defects where regions were attacked forming pits and other regions remained protected after 24 h of immersion in the electrolyte. This result suggested that the coating is better used as a pre-treatment than a final treatment by itself, needing to be used in association with other corrosion protection methods. The needle-like structure observed in the SEM micrographs could grant good anchorage to the surface, allowing it to be possibly used as a paint adhesion promotor similarly to the industrial use of the phosphate layers. The Pechini method stands out as an environmentally friendlier alternative, as the main source of impacts are originated by the energy expenditure to prepare the resin and the fumes from the calcination step, with close to none waste from the process, conversely to the phosphating bath commonly used by industries.

References

- Banczek, E.P., Rodrigues, P.R.P. and Costa, I. (2009), "Evaluation of porosity and discontinuities in zinc phosphate coating by means of voltametric anodic dissolution (VAD)", *Surface and Coatings Technology*, Vol. 203 No. 9, pp. 1213-1219, doi: [10.1016/j.surfcoat.2008.10.026](https://doi.org/10.1016/j.surfcoat.2008.10.026).
- Banczek, E.P., Terada, M., Rodrigues, P.R.P. and Costa, I. (2010), "Study of an alternative phosphate sealer for replacement of hexavalent chromium", *Surface and Coatings Technology*, Vol. 205 No. 7, pp. 2503-2510, doi: [10.1016/j.surfcoat.2010.09.053](https://doi.org/10.1016/j.surfcoat.2010.09.053).
- Chukwuike, V.I., Rajalakshmi, K. and Barik, R.C. (2021), "Surface and electrochemical corrosion analysis of niobium oxide film formed in various wet media", *Applied Surface Science Advances*, Vol. 4, p. 100079, doi: [10.1016/j.apsadv.2021.100079](https://doi.org/10.1016/j.apsadv.2021.100079).
- Cui, J., Yao, Z., Cheng, F., Xiao, T., Sun, H., Tian, R. and Sun, J. (2016), "Electrochemical properties of tungsten-alloying modified AISI460 stainless steel as bipolar plates for PEMFCs used in marine environment", *Acta Metallurgica Sinica*, Vol. 29 No. 10, pp. 920-927.
- Cui, J., Jing, B., Xu, X., Wang, L., Cheng, F., Li, S., Wen, S., Ji, S. and Sun, J. (2017a), "Performance of niobium nitride-modified AISI316L stainless steel as bipolar plates for direct formic acid fuel cells", *International Journal of Hydrogen Energy*, Vol. 42 No. 16, pp. 11830-11837, doi: [10.1016/j.ijhydene.2017.02.145](https://doi.org/10.1016/j.ijhydene.2017.02.145).
- Cui, Y.F., Cui, J.L., Xu, X., Cheng, F.P., Wang, L.X., Li, S., Ji, S.J. and Sun, J.C. (2017b), "Electrochemical properties of niobium modified AISI316L stainless steel bipolar plates for

- direct formic acid fuel cell”, *Fuel Cells*, Vol. 17 No. 5, pp. 698-707, doi: [10.1002/face.201700010](https://doi.org/10.1002/face.201700010).
- Detlinger, P., Utri, B. and Banczek, E.P. (2019), “Corrosion resistance of niobium-coated carbon steel”, *Journal of Bio- and Tribo-Corrosion*, Vol. 5 No. 1, pp. 1-8, doi: [10.1007/s40735-018-0201-9](https://doi.org/10.1007/s40735-018-0201-9).
- Detlinger, P., Helleis, R., Matheus, A.P.C., Utri, B., Dias, B.V., Oliszeski, D.C.S. and Banczek, E.P. (2020), “Study of the corrosion of carbon steel (SAE 1020) coated with niobium oxides”, *Materials Science Forum*, Vol. 1012, pp. 385-389, doi: [10.4028/www.scientific.net/MSF.1012.385](https://doi.org/10.4028/www.scientific.net/MSF.1012.385).
- Dias, B.V., Tractz, G.T., Viomar, A., Maia, G.A.R., Cunha, M.T. and Rodrigues, P.R.P. (2018), “Photo electrochemical behavior of the cell FTO/TiO₂/CeO₂/N719 obtained from the Pechini and precipitation of cerium oxides methods”, *Journal of Electronic Materials*, Vol. 47 No. 9, pp. 5556-5563, doi: [10.1007/s11664-018-6465-5](https://doi.org/10.1007/s11664-018-6465-5).
- Farag, A.A., Ismail, A.S. and Migahed, M.A. (2015), “Inhibition of carbon steel corrosion in acidic solution using some newly polyester derivatives”, *Journal of Molecular Liquids*, Vol. 211, pp. 915-923, doi: [10.1016/j.molliq.2015.08.033](https://doi.org/10.1016/j.molliq.2015.08.033).
- Ferreira, M.O.A., Gelamo, R.V., Marino, C.E.B., Silva, B.P., Aoki, I.V., Luz, M.S., Alexopoulos, N.D., Leite, N.B. and Moreto, J.A. (2022), “Effect of niobium oxide thin film on the long-term immersion of the 2198-T851 aluminium alloy”, *Materialia*, Vol. 22, p. 101407, doi: [10.1016/j.mtla.2022.101407](https://doi.org/10.1016/j.mtla.2022.101407).
- Hartwig, A., Klein, O. and Karl, H. (2017), “Sputtered titanium dioxide thin films for galvanic corrosion protection of AISI 304 stainless steel coupled with carbon fiber reinforced plastics”, *Thin Solid Films*, Vol. 621, pp. 211-219, doi: [10.1016/j.tsf.2016.12.002](https://doi.org/10.1016/j.tsf.2016.12.002).
- Helleis, R., Matheus, A.P.C., Gallina, A.L., Dias, B.V., Maia, G.A.R., Rodrigues, P.R.P. and Banczek, E.P. (2021), “Characterization of a niobium and titanium oxides coatings for the protection of carbon steel SAE 1020”, *Journal of Engineering Research*, Vol. 1 No. 1, pp. 1-10, doi: [10.22533/at.ed.3172115102](https://doi.org/10.22533/at.ed.3172115102).
- Hou, Y., Aldrich, C., Lepkova, K., Machuca, L.L. and Kinsella, B. (2016), “Monitoring of carbon steel corrosion by use of electrochemical noise and recurrence quantification analysis”, *Corrosion Science*, Vol. 112, pp. 63-72, doi: [10.1016/j.corsci.2016.07.009](https://doi.org/10.1016/j.corsci.2016.07.009).
- Huang, H., Wang, H., Xie, Y., Dong, D., Jiang, X. and Zhang, Z. (2019), “Incorporation of boron nitride nanosheets in zinc phosphate coatings on mild steel to enhance corrosion resistance”, *Surface and Coatings Technology*, Vol. 374, pp. 935-943, doi: [10.1016/j.surfcoat.2019.06.082](https://doi.org/10.1016/j.surfcoat.2019.06.082).
- Im, M., Kweon, S., Kim, J., Nahm, S., Choi, J. and Hwang, S. (2014), “Microstructural variation and dielectric properties of KTiNbO₅ and K₃Ti₅NbO₁₄ ceramics”, *Ceramics International*, Vol. 40 No. 4, pp. 5861-5867, doi: [10.1016/j.ceramint.2013.11.028](https://doi.org/10.1016/j.ceramint.2013.11.028).
- Kim, S., Kim, J.W. and Kim, J.H. (2017), “Enhancement of corrosion resistance in carbon steels using nickel-phosphorous/titanium dioxide nanocomposite coating under high-temperature flowing water”, *Journal of Alloys and Compounds*, Vol. 698, pp. 267-275, doi: [10.1016/j.jallcom.2016.12.027](https://doi.org/10.1016/j.jallcom.2016.12.027).
- Li, K., Li, Y., Huang, X., Gibson, D., Zheng, Y., Liu, J., Sun, L. and Fu, Y.Q. (2017), “Surface microstructures and corrosion resistance of Ni-Ti-Nb shape memory thin films”, *Applied Surface Science*, Vol. 414, pp. 63-67, doi: [10.1016/j.apsusc.2017.04.070](https://doi.org/10.1016/j.apsusc.2017.04.070).
- Liu, Y., Lang, Z., Cui, J. and Na, S. (2021), “Performance of Nb_{0.8}Zr_{0.2} layer-modified AISI430 stainless steel as bipolar for direct formic acid fuel cells”, *Acta Metallurgica Sinica (English Letters)*, Vol. 34 No. 1, pp. 77-84, doi: [10.1007/s40195-020-01133-w](https://doi.org/10.1007/s40195-020-01133-w).
- McMahon, R.E., Ma, J., Verkhoturov, S.V., Munos-Pinto, D., Karaman, I., Rubitschek, F., Maier, H.J. and Hahn, M.S. (2012), “A comparative study of the cytotoxicity and corrosion resistance of nickel-titanium and titanium-niobium shape memory alloys”, *Acta Biomaterialia*, Vol. 8 No. 7, pp. 2863-2870, doi: [10.1016/j.actbio.2012.03.034](https://doi.org/10.1016/j.actbio.2012.03.034).
- Matos, L.A.C., Taborda, M.C., Alves, G.J.T., Cunha, M.T., Banczek, E.P., Oliveira, M.F., D’Elia, E. and Rodrigues, P. R.P. (2018), “Application of an acid extract of barley agro-industrial waste as a corrosion inhibitor for stainless steel AISI 304 in H₂SO₄”, *International Journal of Electrochemical Science*, Vol. 13, pp. 1577-1593, doi: [10.20964/2018.02.01](https://doi.org/10.20964/2018.02.01).
- Mofidabadi, A.H.J., Bahlakeh, G. and Ramezanzadeh, B. (2021), “Anti-corrosion performance of the mild steel substrate treated by a novel nanostructure europium oxide-based conversion coating: electrochemical and surface studies”, *Colloids and Surfaces A: Physicochemical and Engineering Aspects*, Vol. 609, p. 125689, doi: [10.1016/j.colsurfa.2020.125689](https://doi.org/10.1016/j.colsurfa.2020.125689).
- Nazeer, A.A. and Madkour, M. (2018), “Potential use of smart coatings for corrosion protection of metals and alloys: a review”, *Journal of Molecular Liquids*, Vol. 253, pp. 11-22, doi: [10.1016/j.molliq.2018.01.027](https://doi.org/10.1016/j.molliq.2018.01.027).
- Orjuela, G.A., Rincón, R. and Olaya, J.J. (2014), “Corrosion resistance of niobium carbide coatings produced on AISI 1045 steel via thermo-reactive diffusion deposition”, *Surface and Coatings Technology*, Vol. 259, pp. 667-675, doi: [10.1016/j.surfcoat.2014.10.012](https://doi.org/10.1016/j.surfcoat.2014.10.012).
- Pan, T.J., Chen, Y., Zhang, B., Hu, J. and Li, C. (2016), “Corrosion behavior of niobium coated 304 stainless steel in acid solution”, *Applied Surface Science*, Vol. 369, pp. 320-325, doi: [10.1016/j.apsusc.2016.02.088](https://doi.org/10.1016/j.apsusc.2016.02.088).
- Pillis, M.F., Geribola, G.A., Scheidt, G., Araújo, E.G., Oliveira, M.C.L. and Antunes, R.A. (2016), “Corrosion of thin, magnetron sputtered Nb₂O₅ films”, *Corrosion Science*, Vol. 102, pp. 317-325, doi: [10.1016/j.corsci.2015.10.023](https://doi.org/10.1016/j.corsci.2015.10.023).
- Pradhan, D., Wren, A.W., Mixture, S.T. and Mellott, N.P. (2016), “Investigating the structure and biocompatibility of niobium and titanium oxides as coatings for orthopedic metallic implants”, *Materials Science and Engineering: C*, Vol. 58, pp. 918-926, doi: [10.1016/j.msec.2015.09.059](https://doi.org/10.1016/j.msec.2015.09.059).
- Robin, A. (2004), “Corrosion behaviour of niobium in sodium hydroxide solutions”, *Journal of Applied Electrochemistry*, Vol. 34 No. 6, pp. 623-629, doi: [10.1023/B:JACH.0000021924.82854.71](https://doi.org/10.1023/B:JACH.0000021924.82854.71).
- Rodrigues, P.R.P., Terada, M., Junior, O.R.A., Lopes, A.C., Costa, I. and Banczek, E.P. (2014), “Niobium pentoxide coating replacing zinc phosphate coating”, *Matéria (Rio De Janeiro)*, Vol. 19 No. 2, pp. 105-116, doi: [10.1590/S1517-70762014000200005](https://doi.org/10.1590/S1517-70762014000200005).

- Santos Júnior, A.G., Antonini, L.M., Sampaio, E.J.P., Andrade, A.M.H., Aguzzoli, C. and Malfatti, C.F. (2022), "Sodium niobates and protonic nanowires obtained from hydrothermal synthesis: electrochemical behavior in aqueous electrolyte", *Ceramics International*, Vol. 48 No. 2, pp. 1522-1531, doi: [10.1016/j.ceramint.2021.09.230](https://doi.org/10.1016/j.ceramint.2021.09.230).
- Sowa, M., Worek, J., Dercz, G., Korotin, A.I.K., Kuhkarenko, A.I., Kurmaev, E.Z., Cholakh, S.O., Basiaga, M. and Simka, W. (2016), "Surface characterization and corrosion behaviour of niobium treated in a Ca- and P-containing solution under sparking effects", *Electrochimica Acta*, Vol. 198, pp. 91-103, doi: [10.1016/j.electacta.2016.03.069](https://doi.org/10.1016/j.electacta.2016.03.069).
- Tao, F., Baoguo, L., Binghui, D., Wei, S., Jitang, F. and Yuan, G. (2014), "Hydrothermal surface modification of a low modulus Ti-Nb based alloy", *Rare Metal Materials and Engineering*, Vol. 43 No. 2, pp. 291-295, doi: [10.1016/S1875-5372\(14\)60061-8](https://doi.org/10.1016/S1875-5372(14)60061-8).
- Tegner, B.E., Zhu, L., Siemers, C., Saksli, K. and Ackland, G.J. (2015), "High temperature oxidation resistance in titanium-niobium alloys", *Journal of Alloys and Compounds*, Vol. 643, pp. 100-105, doi: [10.1016/j.jallcom.2015.04.115](https://doi.org/10.1016/j.jallcom.2015.04.115).
- Tractz, G.T., Luz, F.S., Antunes, S.R.M., Cunha, M.T. and Rodrigues, P.R.P. (2021), "Nb₂O₅ synthesis and

- characterization by the Pechini method to the application as electron transport material", *Solar Energy*, Vol. 216, pp. 1-6, doi: [10.1016/j.solener.2021.01.029](https://doi.org/10.1016/j.solener.2021.01.029).
- Trino, L.D., Dias, L.F.G., Albano, L.G.S., Bronze-Uhle, E.S., Rangel, E.C., Graeff, C.F.O. and Lisboa-Filho, P.N. (2018), "Zinc oxide surface functionalization and related effects on corrosion resistance of titanium implants", *Ceramics International*, Vol. 44 No. 4, pp. 4000-4008, doi: [10.1016/j.ceramint.2017.11.195](https://doi.org/10.1016/j.ceramint.2017.11.195).
- Zhang, H., Jiang, K., Qiu, Y., Man, J., Cui, J., Du, Y., Li, S. and Sun, J. (2019), "Electrochemical properties of niobium and niobium compounds modified AISI430 stainless steel as bipolar plates for DFAFC", *Surface Engineering*, Vol. 35 No. 11, pp. 1009-1011, doi: [10.1080/02670844.2019.1611707](https://doi.org/10.1080/02670844.2019.1611707).
- Zhao, Y., Zhang, Z., Yu, L. and Jiang, T. (2017), "Hydrophobic polystyrene/electro-spun polyaniline coatings for corrosion protection", *Synthetic Metals*, Vol. 234, pp. 166-174, doi: [10.1016/j.synthmet.2017.11.005](https://doi.org/10.1016/j.synthmet.2017.11.005).

Corresponding author

Rodrigo Helleis can be contacted at: rodrigohelleis@gmail.com